

---

## Ontogenetic dietary shifts of the medusa *Rhizostoma pulmo* (Cnidaria: Scyphozoa)

Leoni Valentina <sup>1,\*</sup>, Molinero Juan-Carlos <sup>2</sup>, Crochemore Sandrine <sup>1</sup>, Meffre Marie <sup>1</sup>, Bonnet Delphine <sup>1</sup>

<sup>1</sup> MARBEC, Univ. Montpellier, CNRS, Ifremer, IRD, Montpellier, France

<sup>2</sup> MARBEC, IRD, CNRS, Ifremer, Univ. Montpellier, Sète, France

\* Corresponding author : Valentina Leoni, email address : [valentina.leoni@umontpellier.fr](mailto:valentina.leoni@umontpellier.fr)

---

### Abstract :

Identifying ontogenetic changes in jellyfish diet is fundamental to understand trophic interactions during their life cycle. Scyphomedusae blooms exert major predation pressure on plankton communities, although their role in ecosystems has long been misrepresented. This study assesses seasonal and ontogenetic changes in the diet of the scyphomedusa *Rhizostoma pulmo*, one of the largest yet overlooked Mediterranean jellyfish. Medusae gut contents (n = 127) were collected during one year in Bages Sigean lagoon, southern France. Results show that the diet composition differs from the availability of prey in the environment with contrasting preferences along ontogeny. Calanoid (70%) and harpacticoid (45.8%) copepods were the most frequent prey and the major carbon contributors for small medusae (bell diameter < 15 cm). In contrast, ciliates (43.5%) were the most frequent prey for large organisms (> 15 cm), which obtain most of their carbon intake from ciliates and fish eggs (20.9%). The overall impact on micro and mesozooplankton showed that small medusae consume 5% of the copepods daily standing stock, while large medusae consumed 8% of ciliates daily standing stock. Our results stress that *R. pulmo* display different trophic pathways along its life cycle, firstly interacting with the classical food web, and shifting afterwards to a greater interaction with the microbial loop.

**Keywords :** Gut content, Barrel jellyfish, Mediterranean Sea, Developmental stages

## 58 **Introduction**

59 Assessing the trophic role of species, i.e., what they eat and in what proportions, is fundamental to  
60 understand energy fluxes and ecosystem functioning (Cury et al., 2008). In marine ecosystems,  
61 gelatinous zooplankton are increasingly recognized as conspicuous prey (Hays et al., 2018), consumers  
62 (Robinson & Graham, 2014), and prominent players in biogeochemical cycles (Lebrato et al., 2019).  
63 Cnidarians represent approximately 92% of the total global biomass of gelatinous zooplankton (Lucas et  
64 al., 2014), with scyphomedusae species developing the largest individual body weight and forming  
65 spectacular blooms (Dawson & Hamner, 2009). Due to their voracity on lower trophic levels (Purcell,  
66 1992), scyphomedusae blooms impact the whole food web structure in coastal marine ecosystems,  
67 thereby shaping the ecosystem functioning and services (West et al., 2009).

68 Despite the central role of scyphomedusae and their impact on local economies (e.g., Bosch-  
69 Belmar et al., 2021), the trophic ecology of this taxon is often misrepresented, as the large majority of  
70 studies have focused on two genera, *Aurelia* and *Chrysaora*. The remaining 85% of scyphomedusae  
71 species are overlooked. Consequently, ecosystem models have historically oversimplified their role as  
72 predators (Pauly et al., 2009), although recent evidence has shown a wide variation in their trophic role  
73 which changes not only across species, but also throughout their ontogeny (Fleming et al., 2015).

74 During their life cycle, scyphozoans display a wide range of sizes, from few millimeters up to 1  
75 meter. The few studies that have addressed their ontogenetic dietary shifts have identified diverse  
76 responses. For instance, benthic and pelagic stages trophic niches of some species widely overlap  
77 (*Aurelia coerulea* von Lendenfeld, 1884: Marques et al., 2021), others shift their trophic level with size  
78 (*Lychnorhiza lucerna* Haeckel, 1880: Nagata et al., 2015 and *Cyanea nozakii* Kishinouye, 1891: Wang  
79 et al., 2020), or modify prey preferences and diversity (*Stomolophus meleagris* Agassiz, 1860 and *Aurelia*  
80 *aurita* (Linnaeus, 1758): Larson, 1991; Graham & Kroutil, 2001; Álvarez-Tello et al., 2016). Such diet  
81 changes have been associated with shifts in mouth size, prey encounter probability, or small-scale  
82 currents generated by bell pulsations (Costello & Colin, 1995; Nagata et al., 2016).

83 Among the methods used to determine the trophic role, four have been implemented on  
84 scyphozoans' diet analyses (Pitt et al., 2009): i.e., gut content, grazing experiments, stable isotope (SI)  
85 and fatty acid (FA) analyses. SI and FA analyses provide the signal of the assimilated food, but require a  
86 previous knowledge of the prey's signal in the environment (Pitt et al., 2009). In turn, gut content analysis  
87 provides information on recently ingested food, although it does not allow detecting the assimilated one,  
88 and therefore underestimate preys that are digested rapidly (e.g., Purcell, 1997; Båmstedt & Martinussen,  
89 2000). Notwithstanding this limitation, it remains the most direct method for prey identification (Purcell,

90 2018). A protocol to standardize the assessment of scyphomedusae gut content has been only recently  
91 provided (Nagata & Morandini, 2018). To date, however, gut content analyses on jellyfish have generally  
92 based their conclusions on a small sample size, and overlooked the predators and prey seasonality, which  
93 are not only crucial to define dietary niches but are also essential to incorporate this group in food web  
94 models.

95 By virtue of their relative shallowness and protection from the open sea, semi-enclosed  
96 ecosystems, such as coastal lagoons, are exceptional places to study jellyfish trophic interactions in  
97 natural environments (Marques et al., 2021). Bages Sigean (France) (43°05'12.72" N; 3°00'35.3" E) is  
98 a small Mediterranean coastal lagoon (38 km<sup>2</sup>, mean depth of 2 m) located in a protected area (Cesmat  
99 et al., 2012). The lagoon is a shelter for migrant birds and fishes, and an important biodiversity reservoir  
100 (PNRNM, 2018), where a perennial population of the barrel jellyfish *Rhizostoma pulmo* (Macri, 1778)  
101 has been detected since 2014.

102 *R. pulmo* is a native Rhizostomeae scyphomedusa from the Mediterranean and Black Seas (Leoni  
103 et al., 2021a). This scyphomedusa can reach biomasses of 300 tons km<sup>-2</sup> during bloom events (Basso et  
104 al., 2019), with dramatic effects on fisheries (Nastav et al., 2013) and potentially on the food web  
105 structure (e.g., Brodeur et al., 2002). In Bages Sigean, summer blooms of *R. pulmo* (Leoni et al., 2021b)  
106 are a major issue for artisanal fishing due to net clogging, spoiling the commercial value of captured fish  
107 and because of the risk of stings (S. Marin pers. comm.). Similar problems have been reported in other  
108 ecosystems inhabited by this species, such as Mar Menor lagoon (Spain) (Fuentes et al., 2011).

109 The feeding mechanism of *R. pulmo* is peculiar. Instead of a central mouth, such as in *Aurelia* and  
110 *Chrysaora*, Rhizostomeae medusae have eight specialized oral arms covered with millimetric mouths  
111 where the food is ingested due to micro-currents generated by bell pulsation (Nagata et al., 2016).  
112 However, little is known about the diet of this species (Pérez-Ruzafa et al., 2002; Dönmez & Bat, 2019).

113 In this study, we benefited from the large size range of individuals present across the year in Bages  
114 Sigean lagoon (Leoni et al., 2021b) to assess *R. pulmo* diet throughout the pelagic stages. Owing to the  
115 medusa mouths size (ca. 3,000 µm), we hypothesized (H1) a diet mainly composed by a dominance of  
116 small prey. In addition, as it is expected that prey encounter rate and micro-currents generated by bell  
117 pulsations increase along medusa ontogeny (Nagata et al., 2016), we hypothesized an increase of prey  
118 richness (H2) and mobile prey (H3) in the diet along with medusa growth. By means of gut content  
119 analysis, we (1) describe prey diversity and size range during ontogeny, (2) quantify prey relative  
120 abundance, (3) examine potential prey-selectivity patterns of the species, and (4) identify the main  
121 sources of carbon supply during ontogeny, as well as its predatory impact in the lagoon.

## 122 **Materials and Methods**

123 Biological samples were gathered biweekly between February and November 2019 in Bages Sigean  
124 lagoon (see Figure 1 in Leoni et al., 2021b) between 09:00 and 12:00 AM. The abundances of *R. pulmo*  
125 pelagic stages were estimated using two complementary sampling procedures. Young individuals were  
126 caught with a 700- $\mu$ m mesh size plankton net fitted with a flowmeter, which was towed horizontally at  
127 the sub-surface due to the shallowness of the lagoon. In turn, the abundance of large organisms was  
128 estimated with a non-intrusive method of visual counting from the boat (Leoni et al., 2021b). Abundance  
129 estimations were expressed as the number of medusae per 100 cubic meters.

130

### 131 *Jellyfish gut content analysis*

132 *R. pulmo* medusae size classes were defined based on the absence (juveniles) or presence (adults) of  
133 gonads. We used 15 cm as the bell diameter (BD) threshold to distinguish juveniles from adults'  
134 specimens, as gonads were present in all individuals with BD >15 cm.

135 The methodology applied to assess the medusae gut content was based on Nagata & Morandini  
136 (2018). Medusa specimens were carefully collected by dip nets from the boat. Only unharmed and active  
137 individuals were considered. BD ( $\pm 0.05$  cm) and wet weight (WW  $\pm 0.05$  kg) of the specimens were  
138 recorded. Each medusa was stored individually in a plastic jar with formalin 10%. In the laboratory,  
139 medusae were singly laid down on a tray and methylene blue was injected into the specimens' gut to  
140 facilitate prey visualization (Nagata & Morandini, 2018). Later, oral arms were removed by scissors and  
141 the cruciform gut was opened. The cavity was rinsed with 0.2  $\mu$ m filtered seawater and the washed  
142 content was retained on a 63- $\mu$ m sieve. Consequently, 63- $\mu$ m was the lower size threshold of prey  
143 identification. The gut walls were also examined under a Leica stereomicroscope to collect prey  
144 eventually retained therein. Both, prey items removed by rinsing and those attached to the gastric cirri  
145 were conserved in formalin 4% and included in counts.

146 Prey items were identified and counted in a Bogorov chamber under a stereomicroscope. When  
147 possible, specimens were identified at species or genus level. Otherwise, identification was carried out  
148 to the greatest detail possible. Phytoplankton was counted but was not considered for the analyses as it  
149 was probably underestimated due to the minimal size of prey identification. Individual prey  
150 measurements were determined from pictures with a camera integrated into the stereomicroscope, using  
151 the software Leica Application Suite X (LAS X). Schematic representations of how measurements were  
152 taken are presented in Figure S1, mainly following Uye (1982).

153

154 *Characterization of food availability*

155 To characterize the zooplankton community and to evaluate *R. pulmo* prey selectivity patterns,  
156 zooplankton and medusae collections were performed simultaneously. Micro-, meso- and  
157 macrozooplankton were collected with 63- $\mu\text{m}$  (0.40 m diameter x 1.00 m length), 200- $\mu\text{m}$  (0.54 m  
158 diameter x 2.50 m length) and 700- $\mu\text{m}$  (0.78 m diameter x 2.00 m length) mesh size plankton nets,  
159 respectively, each fitted with a flowmeter and towed horizontally in the sub-surface layer. Samples were  
160 fixed in formalin 4%. Two samples were taken for meso- and macrozooplankton in the study area at each  
161 sampling date, while only one sample was collected for microzooplankton at each date.

162 Microzooplankton was analyzed with a FlowCam imaging system (Fluid Imaging Inc.; Sieracki  
163 et al., 1998) at the Villefranche Oceanography Laboratory, LOV, while the posterior classification was  
164 performed in EcoTaxa. Data are available online (<https://ecotaxa.obs-vlfr.fr/prj/3279>). Meso- and  
165 macrozooplankton organisms were counted and identified under the stereomicroscope using taxonomic  
166 guides (Trégouboff & Rose, 1978; Hecq et al., 2014). Zooplankton abundances were estimated from  
167 subsamples and expressed as individuals per cubic meter.

168

169 Statistical analysis

170 To characterize and quantify the diet of *R. pulmo*, each medusa was treated as a sampling unit. In addition,  
171 to allow future comparative analyses, we used standard equations and nomenclature employed in trophic  
172 indices assessments, as summarized in da Silveira et al. (2020).

173

174 *Assessing the minimum sample size*

175 A cumulative curve of the number of medusae analyzed against the number of prey taxa in the guts was  
176 used to determine adequate sample size, i.e., the minimum number of samples (*MNS*) to represent the  
177 total richness. We used the Chao1 non-parametric estimator ( $S_{Chao1}$ ):

178 
$$S_{Chao1} = S_{obs} + \frac{n_1^2}{2n_2}$$

179 where  $S_{obs}$  is the observed richness,  $n_1$  is the number of species found once, and  $n_2$  is the number of  
180 species found twice (Chao et al., 2009). The sampling effort was considered sufficient when  $S_{obs}$  was  
181 equal to 80% of  $S_{Chao1}$  (Jiménez-Valverde & Hortal, 2003). This analysis was performed in the software  
182 R using the *rarc* function of the 'rich' package (Rossi, 2011).

183

184 *Objective 1. Prey's richness and frequency of occurrence during R. pulmo ontogeny*

185 To evaluate whether changes during ontogeny were related to changes in prey's richness, the number of  
186 prey taxa found in juvenile and adult medusae was compared using a Kruskal-Wallis test. A significance  
187 level of 5% was applied. In addition, the proportion (%) of empty guts ( $G_e$ ) was estimated by month per  
188 stage of development.

189 The frequency of occurrence ( $FO$  in %) of a prey category ( $i$ ) in the gut content of both juvenile  
190 and adult medusae was estimated as the number of guts with this food item ( $G_i$ ) over the total number of  
191 guts containing food ( $G_f$ ) (da Silveira et al., 2020).

192  
193 *Objective 2. Relative abundance of prey on the diet of R. pulmo pelagic life stages*

194 The percentage of the relative abundance ( $N$ ) of prey was calculated for each prey taxa for all medusae  
195 containing food. The average relative abundance was determined by month for both stages of  
196 development.  $N$  (%) was estimated as the number of individuals of a prey category ( $N_i$ ) over the total  
197 number of prey items found in the medusa gut ( $\sum N_i$ ) (Hyslop, 1980):

198 
$$\%N = \left( \frac{N_i}{\sum_{x=1}^i N_i} \right) * 100$$

199  
200 *Trophic niche determination*

201 The trophic niche breadth ( $NB$ ) was estimated for juveniles and adults medusae using Levin's standardized  
202 index (Krebs, 1999):

203 
$$NB_k = \frac{1}{n - \left( \frac{1}{\sum p_{ik}^2} - 1 \right)}$$

204 where  $NB_k$  is Levin's standardized index for a predator  $k$ ;  $p_{ik}$  is the proportion of a prey  $i$  in the diet of  
205 the predator  $k$ , and  $n$  is the number of prey categories. This index ranges from 0 to 1, where low values  
206 represent a narrow niche breadth or a specialized diet, whilst higher values suggest a generalist diet with  
207 a wide niche breadth.

208 Lastly, we assessed the niche overlap between juveniles and adults when they coexist. This metric  
209 was expressed as the percentage of similarity between juveniles' ( $j$ ) and adults' ( $a$ ) diets, and estimated  
210 with the simplified Morista's index of similarity ( $NO$ ) (Krebs, 1999):

211 
$$NO = 2 * \frac{\sum (P_{ij} * P_{ia})}{\sum P_{ij}^2 + \sum P_{ia}^2}$$

212 Here,  $P_{ij}$  and  $P_{ia}$  are the proportions of the resource  $i$  used respectively by juveniles and adults in relation  
213 to the total resources. The values ranged from 0 to 100%, with 0% representing no diet overlap, and 100%

214 identical diets. We followed the criteria of Langton (1982), and determined three categories of niche  
215 overlap: low (<29%), medium (30-60%) and high (>60%). This index is sensitive to the taxonomic  
216 resolution of preys identified. Here, differences at the species level, if they exist, were not considered in  
217 the niche overlap evaluation.

218

### 219 *Objective 3. Prey selectivity patterns during R. pulmo ontogeny*

220 To account for differences in the relative abundance ( $N$ ) of a prey type ( $i$ ) in the gut ( $G_i$ ) vs prey in the  
221 environment ( $E_i$ ), we used the linear food selection index ( $LFSI$ ) (Strauss, 1979). ‘Positive selection’ was  
222 considered when the  $G_i$  was higher than  $E_i$ , and ‘negative selection’ when  $G_i$  was lower than  $E_i$ .  $LFSI$   
223 was estimated per medusa. Values of  $LFSI$  range from -1 to 1, reflecting the magnitude of prey selection.  
224 Null values indicate no selection, positive values suggest some degree of positive selection and negative  
225 values have a probable disability to consume the prey, i.e., negative selection. To evaluate whether  
226 seasonal and/or ontogenetic changes were related to changes in prey selectivity patterns, a heatmap of  
227  $LFSI$  was performed by month and by medusae size range (BD in cm) for each type of prey. Size classes  
228 of 5 cm were set up with juveniles including the classes 0-5, 5-10 and 10-15 cm, and adults the classes  
229 15-20, 20-25, 25-30 and >30 cm.

230

### 231 *Objective 4: Daily Carbon Ration (DCR) assessment and predatory impact*

232 The daily ration ( $DR$ ) was estimated as the number of prey consumed ( $P_c$ ) by medusa per day as:

233

$$DR = P_c * 24 * DT^{-1}$$

234 using the digestion time ( $DT$ , in hours) for each prey provided in Larson (1991) (Table S1) and corrected  
235 by temperature as follows:

236

$$DT_t = 1 * (DT * Q_{10}^{(t-29)/10})^{-1}$$

237 where  $t$  is the temperature at each sampling date and  $Q_{10}$  was assumed equal to 2.08 (Purcell, 2009).  
238 Lastly,  $DR$  was converted to daily carbon ration ( $DCR$ ) by multiplying  $P_c$  by the carbon content ( $C$  in  
239 mg) estimated for each prey using specific equations (Table S1).  $DCR$  was estimated for prey items found  
240 in more than 5% of samples. We used a biometric conversion factor estimating  $C$  as a percentage of  $R$ .  
241 *pulmo*'s WW:  $C\%WW = 0.34$  (Purcell et al., 2010) to estimate the  $C$  content of each medusa (WW range:  
242 0.25 to 2761g). Quantile regressions (5<sup>th</sup>, 50<sup>th</sup> and 95<sup>th</sup>) were used to evaluate possible changes in carbon  
243 sources with medusae size (mgC) (Cade & Noon, 2003).

244 Based on medusae abundances, the predatory impact of *R. pulmo* in the lagoon was estimated as  
245  $PI = DR * (D_{pred} * D_{prey}^{-1}) * 100$ , where  $PI$  is the percentage of the prey standing stock consumed by the

246 medusae population per day,  $D_{\text{pred}}$  is the abundance of medusae ( $\text{ind m}^{-3}$ ) and  $D_{\text{prey}}$  the abundance of the  
247 prey in the environment ( $\text{ind m}^{-3}$ ) (Nagata & Morandini, 2018). PI was estimated for juveniles and adults  
248 by prey taxa.

249

250 All the analyses were performed using the open source software R 3.6.0 (R Core Team, 2020)  
251 and plots were created with the 'ggplot2' package (Wickham, 2016).



## 252 **Results**

### 253 *Jellyfish population dynamics*

254 In total, 16 samplings were performed. Ephyrae and small medusae appeared for the first time in April  
255 and the last medusae were observed in October. The seasonal dynamics of *R. pulmo* pelagic stages  
256 showed a maximum abundance in April and two smaller peaks in June and July (Fig. 1a). Ephyrae  
257 occurred from April to June, juveniles from April to September, and adults from May to October.  
258 Maximum abundances of ephyrae, juveniles and adults medusae were observed in June (6.1 ind 100 m<sup>-3</sup>)  
259 <sup>3</sup>), April (17.5 ind 100 m<sup>-3</sup>) and June (1.0 ind 100 m<sup>-3</sup>), respectively. Due to overlapped cohorts, in some  
260 months, more than one developmental stage was present. The first cohort developed from April to  
261 September, the second cohort from May to October, and the third cohort from June to October. However,  
262 as there were not enough individuals collected from the third cohort, only specimens from the two first  
263 cohorts were considered for gut content analysis (Fig. 1b, c). In total, 127 individuals were collected (Fig.  
264 1b), from May to October, with a BD ranging from 0.95 to 34.00 cm (Fig. 1c) and a WW from 0.25 to  
265 2761.00 g.

266

### 267 *Prey richness*

268 A total of 16,239 prey items were counted in the gut contents, with an average prey concentration of 20  
269  $\pm 22$  prey medusa<sup>-1</sup> in juveniles and 253  $\pm 338$  prey medusa<sup>-1</sup> in adults. After screening, 14 taxa were  
270 assigned into three different prey categories based on size criteria: (i) microzooplankton (63-200  $\mu$ m)  
271 containing: foraminifers (phylum Foraminifera), ciliates (phylum Ciliophora), bivalve and gastropod  
272 veligers (phylum Mollusca), ostracods and copepods' nauplii (phylum Arthropoda), (ii)  
273 mesozooplankton (200-700  $\mu$ m) composed by: cirripeds' nauplii and harpacticoid, cyclopoid and  
274 calanoid copepods (phylum Arthropoda), and (iii) macrozooplankton (>700  $\mu$ m) including:  
275 hydromedusae (phylum Cnidaria), fish eggs (phylum Chordata), crustacean malacostraceans (phylum  
276 Arthropoda) and polychaetes (phylum Annelida). Micro- and mesozooplankton specimens were the most  
277 recurrent prey, while the predominant group by category was the ciliates (20.8%) and the calanoid  
278 copepods (22.8%), respectively. Ciliates were mostly represented by the genus *Codonella*, *Favella*, and  
279 *Tintinnopsis*, whilst calanoid copepods were mostly represented by three species: *Acartia clausi*  
280 Giesbrecht, 1889, *Paracalanus parvus* (Claus, 1863) and *Pseudocalanus elongatus* (Brady, 1865).

281 Our sampling size was representative of the prey richness in *R. pulmo*'s guts. Indeed, the Chao1  
282 non-parametric estimator indicated that the sampling effort can be considered sufficient when analyzing  
283 84 specimens (Fig. 2a), when  $S_{obs}$  (observed richness = 35) is 80% of the  $S_{Chao1}$  (total richness estimated

284 = 39). The number of taxa identified (14 taxa) showed a significant difference between juveniles and  
285 adults ( $df=1$ ,  $p=0.007$ ), with more taxa in adults ( $4.2\pm 2.4$  taxa medusa<sup>-1</sup>) compared to juveniles ( $2.8\pm 1.9$   
286 taxa medusa<sup>-1</sup>) (Fig. 2b).

287         Among the total specimens analyzed, 13% of the medusae guts were judged empty (17 specimens  
288 out of 127). Of them, 10 guts had only items of vegetal origin and the remaining 7 were empty. Vegetal  
289 structures, including *Pinus* pollen grains and stellate hair of vascular plants (i.e., *Elaeagnus* sp.) were  
290 observed in 61.2% of the guts analyzed, but were removed from the analyses as they were considered as  
291 terrestrial contamination. Thus, only 110 individuals were retained for the analyses: 62 juveniles and 48  
292 adults.  $G_e$  (%) displayed a marked temporal variability (Fig. 2c). When *R. pulmo* appeared, more than  
293 30% of juveniles presented empty guts, although no empty guts were observed at the beginning of  
294 summer (June), and only a few (~10%) until September. Conversely, all adults presented food in their  
295 guts from May to July. From July, an increase in the number of empty guts was noted, up to a maximum  
296 in October ( $G_e = 50\%$ ).

297

#### 298 *Objective 1. Frequency of occurrence of prey during R. pulmo ontogeny*

299 The ingested prey covered a size range from 45 to 9,000  $\mu\text{m}$  (Fig. 3a), with most of them (80%) figuring  
300 between 165-240  $\mu\text{m}$ . Prey size varied significantly (Kruskal-Wallis,  $df=1$ ,  $p<0.001$ ) between juvenile  
301 and adult medusae, with juvenile medusae feeding on larger sizes ( $385\pm 190$   $\mu\text{m}$ ) than adult medusae  
302 ( $136\pm 60$   $\mu\text{m}$ ).

303         Calanoid and harpacticoid copepods were, together with ciliates, the most frequent prey (Fig. 3b).  
304 Of them, calanoid copepods doubled their occurrence in juveniles compared to adults, reaching a  $FO=70\%$   
305 in juveniles. Conversely, ciliates, copepods' nauplii and malacostraceans were slightly more frequent in  
306 adults compared to juveniles (Fig. 3b). In general, the biggest prey as malacostraceans, were observed  
307 with a frequency of occurrence ( $FO$ ) lower than 20%. The less consumed items, i.e., ostracods (ca. 130  
308  $\mu\text{m}$ ), hydromedusae (ca. 500  $\mu\text{m}$ ) and polychaetes (ca. 9000  $\mu\text{m}$ ), present in less than 5% of the  
309 specimens, were removed for posterior analyses.

310

#### 311 *Objective 2. Relative abundance of prey in the diet of R. pulmo pelagic life stages*

312 The relative abundance of prey in the gut contents of the medusae did not follow their seasonal abundance  
313 in the environment (Fig. 4). From May to July, the diet of juveniles was composed mainly of calanoid  
314 copepods ( $N>25\%$  each month). In August and September, this composition changed to a predominance  
315 of foraminifera ( $N>25\%$ ), matching with the abundance peak of this group (Fig. 5), and in lower

316 proportion to ciliates and harpacticoid copepods. The predation on fish eggs was noticeable during May  
317 (ca. 20%) and August (8%). In contrast, adults showed a different diet composition, with a predominance  
318 of ciliates, mainly in June (ca. 40%), August ( $N>80\%$ ) and September (ca. 40%), followed by calanoid  
319 and harpacticoid copepods, and bivalve veligers.

320 Trophic niche breadth suggested a specialist feeding behavior for juvenile and adult medusae with  
321 low values in both cases ( $NB_{juveniles}=0.07$ ,  $NB_{adults}=0.08$ ). Most of the time, when juveniles and adults of  
322 different cohorts coexist, the niche overlap was low (13% in June and September, and 22% in May), but  
323 increased to medium or high in August (54%) and July (68%), respectively (Fig. 4). The highest overlap  
324 observed in July was caused by the predominance of bivalve veligers and calanoid copepods in the diet  
325 of both juveniles and adults.

326

### 327 *Objective 3. Prey selectivity patterns during R. pulmo ontogeny*

328 The prey selectivity showed a heterogeneous pattern (Fig. 5). Copepods' nauplii and gastropod veligers  
329 showed a negative selection most of the time, except for a positive selection of gastropod veligers by the  
330 biggest medusae (>30 cm). Foraminifers, calanoid copepods and fish eggs were positively selected by  
331 juvenile medusae during some months. It is worth noticing that calanoid copepods were mostly ingested  
332 by the smallest sizes of *R. pulmo* (<10 cm), while ciliates were selected by adult medusae (>15 cm) (Fig.  
333 5).

334

### 335 *Objective 4: Daily Carbon Ration assessment and predatory impact*

336 The daily carbon ration (*DCR*, mgC consumed per medusa per day) consumed by the medusae differed  
337 between prey types during *R. pulmo* growth (Fig. 6). At the smallest sizes of *R. pulmo* (<34 mgC or <6  
338 cm of BD), copepods were the most consumed prey, with a *DCR* between ca. 0.01 to 1 mgC medusa<sup>-1</sup>  
339 day<sup>-1</sup>, decreasing their maximum consumption (95<sup>th</sup> quantile) on biggest sizes (Fig. 6). Along with  
340 medusae growth (from 10 to 2,761g WW, or 34 to 9,387mgC), prey richness increased. Indeed, 95<sup>th</sup>  
341 quantile regression highlighted significant patterns for ciliates, bivalve veligers, cirripeds' nauplii and  
342 fish eggs (Fig. 6). For all of them, the *DCR* increased from juvenile to adult medusae. Ciliates *DCR*  
343 showed a marked increase in the 95<sup>th</sup> quantile, from ca. 0.01 to 10 mgC medusa<sup>-1</sup> day<sup>-1</sup>. Among mollusks,  
344 bivalve veligers contributed significantly more to adult medusae than to juvenile stages *DCR*, while  
345 gastropods were an important food resource only for the adults. Finally, fish eggs showed an increase in  
346 the mean *DCR* values (50<sup>th</sup> quantile) from ca. 1 mgC medusa<sup>-1</sup> day<sup>-1</sup> in juvenile medusae to 4 mgC  
347 medusa<sup>-1</sup> day<sup>-1</sup> in adults, and with maxima (95<sup>th</sup> quantile) ranging from ca. 2 to 30 in juvenile and adult

348 medusae, respectively. For *R. pulmo*, the prey that mostly contributed to the *DCR* were copepods for  
349 juveniles, and fish eggs and ciliates for adult medusae.

350         The predatory impact of *R. pulmo* differs during ontogeny. Juveniles fed on a maximum of 5% of  
351 the copepods' standing stock per day, whilst adults showed a consumption of 8% of the ciliates' standing  
352 stock per day. Fish eggs (mean diameter  $1170 \pm 126 \mu\text{m}$ ) were consumed with high frequency for juveniles  
353 (40%) and adults (20%) with a consumption of approximately 5% of the fish eggs daily standing stock  
354 in the lagoon. For the other taxa, the ingestion was lower than 1% of the daily standing stock.

355

## 356 **Discussion**

357 We have assessed the diet composition of *R. pulmo* pelagic stages and identified ontogenetic dietary  
358 shifts. In addition, the analysis of two different cohorts allows evaluating the degree of trophic niche  
359 breath overlapping between juveniles and adults. The present study, therefore, provides a baseline to  
360 understand the trophic role of *R. pulmo* in plankton food webs.

361

### 362 *Rhizostoma pulmo* diet composition

363 *R. pulmo* fed on different trophic levels, including ciliates, copepods and larger taxa such as fish eggs.  
364 These observations are in agreement with the diet reported for this species in the Black Sea (Dönmez &  
365 Bat 2019). However, our results contrast with Pérez-Ruzafa et al. (2002) who suggested that *R. pulmo*  
366 feed mainly on prey with no active escape ability (e.g., phytoplankton). Such statement is likely biased  
367 by the small sample size used (n=5). Our results indicate that *R. pulmo* is a selective filter-feeder, although  
368 a wide prey species richness is observed, as for other Rhizostomeae (e.g., Kikinger, 1992; Álvarez-Tello  
369 et al., 2016; Nagata & Morandini, 2018; Syazwan et al., 2021) that also include phytoplankton, as  
370 detected in this study (e.g., diatoms *Bacillaria paxillifer*) and previously documented for *R. pulmo*  
371 (Pérez-Ruzafa et al., 2002; Dönmez & Bat, 2019) and *R. octopus* (Gmelin, 1791) (Hays et al., 2012).

372

### 373 *R. pulmo* prey size spectrum

374 Using the only available study to date (Pérez-Ruzafa et al. 2002), Lilley et al. (2009) determined that *R.*  
375 *pulmo* mostly consume (>80%) small prey (<200 µm). Our results show a wide prey size spectrum, from  
376 45 to 9,000 µm, with 80% of prey belonging to the 165-240 µm window. This size range is expected for  
377 the Rhizostomeae diet due to their small mouths size (<3,000 µm). In Semaestomeae species such as  
378 *Aurelia* and *Chrysaora*, more than 50% of prey are commonly larger than 800 µm (Lilley et al., 2009).  
379 Here, the smaller prey size identified for *R. pulmo* suggests a probable niche partitioning and different  
380 trophic roles between these jellyfish.

381

### 382 Consequences of ontogenetic dietary shifts on jellyfish

383 Ontogenetic dietary shifts are widespread in the animal kingdom (Sánchez-Hernández et al., 2019), and  
384 there is evidence that jellyfish can modify their diet over their life span (e.g., Graham & Kroutil, 2001).  
385 Here, gut content analysis revealed that *R. pulmo* raised prey richness with increasing size of medusae  
386 (supporting our H1), but also fed on specific trophic levels during ontogeny. Juvenile stages of *R. pulmo*  
387 showed a marked preference for calanoid copepods ( $FO > 60\%$ ), whilst the feeding pressure on this taxon

388 decreased when medusae grew. In contrast, an increasing consumption, i.e., daily carbon ration, was  
389 observed mainly on ciliates with medusae growth (see Fig. 6). These different prey preferences during  
390 ontogeny and the observed niche partitioning of *R. pulmo*, can affect medusae growth and survival,  
391 probably with evolutionary advantages for multicohort species. For instance, a niche partitioning  
392 between juvenile and adult medusae could reduce competition for food between cohorts, enabling their  
393 coexistence in the lagoon.

394 From a food web perspective, this ontogenetic diet shift might modify the impact and pressure  
395 across the plankton food web. In shallow areas of the ocean, lakes or lagoons, the classical food web  
396 (large phytoplankton-mesozooplankton-fish) is commonly connected with the microbial food web  
397 (bacteria-heterotrophic flagellates-protists) by mesozooplankton species such as copepods (Moore et al.,  
398 2019). However, mesocosm experiments have shown that gelatinous zooplankton has a top-down control  
399 on both the microbial loop (Turk et al., 2008) and the classic food web (Granéli & Turner, 2002). Our  
400 results support these observations and further quantify the impact on standing stocks of copepods and  
401 ciliates. Juvenile medusae of *R. pulmo* consumed a maximum of 5% of the copepods' daily standing  
402 stock, whilst adults showed a consumption of 8% of the ciliates' daily standing stock. These results are  
403 close to the reported values for the Rhizostomeae *L. lucerna*, for which a consumption of 6 to 12% of  
404 the copepods' daily standing stock was estimated in the southwestern Atlantic coast (Nagata & Morandini,  
405 2018), but smaller than the estimations for the giant Japanese Rhizostomeae *Nemopilema nomurai*  
406 Kishinouye, 1922 (24% of mesozooplankton daily standing stocks) (Uye, 2008). Estimations on  
407 Semaestomeae species present a wider interstudy variability, ranging from <3% of the crustaceans' daily  
408 standing stocks consumed by *Aurelia labiata* Chamisso & Eysenhardt, 1821 and *Cyanea capillata*  
409 (Linnaeus, 1758) in Alaska (Purcell, 2003), to 21% of copepods' daily standing stocks consumed by  
410 *Aurelia solida* Browne, 1905 in Bizerte lagoon (France) (Gueroun et al., 2020). Despite these differences,  
411 we observed that large medusae of *R. pulmo* consumed small percentages of copepods' standing stocks  
412 when compared to younger stages, as described for *C. capillata* (Purcell 2003). These results highlight  
413 that the predatory impact by some jellyfish species on the copepods' community could be relevant only  
414 during the first pelagic stages.

415

#### 416 Potential driving mechanisms of ontogenetic diet changes

417 The high prey richness we detected in large medusae agrees with reports for other scyphomedusae species  
418 (Graham & Kroutil, 2001; Padilla-Serrato et al., 2013; Dönmez & Bat, 2019), and might be related to an  
419 increasing encounter rate of un abundant taxa with the predator. This support our hypothesis H2 regarding

420 a diet diversification on adult stages. In contrast, we do reject our hypothesis H3 about an increase of  
421 mobile prey, e.g., copepods, in medusae guts along with medusa growth.

422 To understand these results, we discuss potential feeding mechanisms below. The food selection  
423 of filter-feeder medusae depends on the pre-encounter and post-encounter feeding mechanisms. Pre-  
424 encounter rates are dependent on current speeds generated by the medusae, escape capacity of the prey,  
425 and encounter rate related to predator-prey abundance and size (Costello & Colin, 1994). In this line, our  
426 results do not follow the proposed functional model for prey selection of *A. aurita* (Costello & Colin  
427 1995), which hypothesized that the largest medusae might capture more efficiently big mobile prey than  
428 juveniles. This explanation is based on the marginal flow speed created by bell pulsation and the increase  
429 of encounter rate, which scale with medusae BD (Costello & Colin, 1994), as observed also in  
430 Rhizostomeae species (Nagata et al., 2016; Graham et al., 2003). Nevertheless, deviations from this  
431 pattern have been already reported. The high presence of copepods in the youngest medusae stages of  
432 *Rhopilema nomadica* Galil, Spanier & Ferguson, 1990 (Kuplik & Angel, 2020), *S. meleagris* (Álvarez-  
433 Tello et al. 2016), *Pelagia noctiluca* (Forsskål, 1775) (Rosa et al., 2013), and also in *A. aurita* (Costello  
434 & Colin, 1994; Graham & Kroutil, 2001), suggests that other mechanisms, besides size, could take place.  
435 For instance, small medusae may not be detected by copepods, which could explain their capture.  
436 Conversely, copepods' ability to detect marginal flow speeds created by large medusae (BD >10 cm)  
437 would result in a low consumption by medusae in adult stage, limiting their trophic impact (Wagner et  
438 al., 2020). Beyond that, a faster metabolism and growth rates observed in the youngest specimens  
439 compared to adult stage is a probable explanation for *R. pulmo* (Leoni et al., 2021b), as previously  
440 suggested for *P. noctiluca* (Rosa et al., 2013).

441 Once the contact is established, the ingestion of the prey depend on the physical constrains of the  
442 feeding structures (Kuplik & Angel, 2020), as well as on the type and amount of nematocysts (Purcell,  
443 1984, 1997, 2003), which suggest that ontogenetic differences partly depend on nematocysts composition  
444 (Purcell & Mills, 1988; Carr & Pitt, 2008; Regula et al., 2009). Broadly, the efficiency of the nematocysts  
445 type varies between 'soft-' vs 'hard-bodied' prey (Purcell, 2003) and has been widely described on  
446 hydromedusae and siphonophores (e.g., Purcell, 1984; Purcell & Mills, 1988; Damian-Serrano et al.,  
447 2021). Also, interspecific variations in the feeding ecology of scyphomedusae with similar bell marginal  
448 flow have been correlated with differences in nematocysts composition (Purcell, 2003), which have been  
449 also observed between stages of development (e.g., planulae, scyphystomeae, ephyrae and medusae) in  
450 some Rhizostomeae and Semaestomae species (reviewed in Calder, 1983). However, a shift in  
451 nematocysts composition or proportion during medusae ontogeny have been only identified in cubozoan

452 species (*Chironex fleckeri* Southcott, 1956 and *Chiropsalmus quadrigatus* Haeckel, 1880) and related  
453 with prey consumption (Carrette et al., 2002; Oba et al., 2004). In both cases, ontogenetic shifts from a  
454 crustacean dominant diet ('hard-bodied' prey) to a fish diet ('soft-bodied' prey) were observed. To our  
455 knowledge, only one recent study has analyzed those changes on scyphomedusae (*P. noctiluca*;  
456 Ballesteros et al., 2021), while ontogenetic shifts in nematocysts composition remains unknown for *R.*  
457 *pulmo*. In our study, the observations could be related to shifts in hydrodynamics and encounter rates  
458 (Costello & Colin, 1994), predator-prey behavior (Graham & Kroutil, 2001), or to ontogenetic changes  
459 of nematocysts composition.

460

#### 461 Recommendations for future jellyfish gut content analysis

462 The gut content analysis of a wide range of medusae sizes has provided novel information on the trophic  
463 ecology of *R. pulmo* medusae stages. Our suggestion is that jellyfish diet and their influence on the food  
464 web should consider all stages of development. Moreover, to identify all potential prey, the use of  
465 biochemical markers must be implemented (e.g., Marques et al., 2021). This is particularly important on  
466 small prey as phytoplankton, microplankton smaller than 63  $\mu\text{m}$  and detritus, already identified as  
467 important food items for some jellyfish species. Despite the limitations of direct gut content analysis, this  
468 technique provides a baseline for posterior SI analyses (Pitt & Lucas, 2013) and it is the unique approach  
469 for which the size of the prey can be measured.

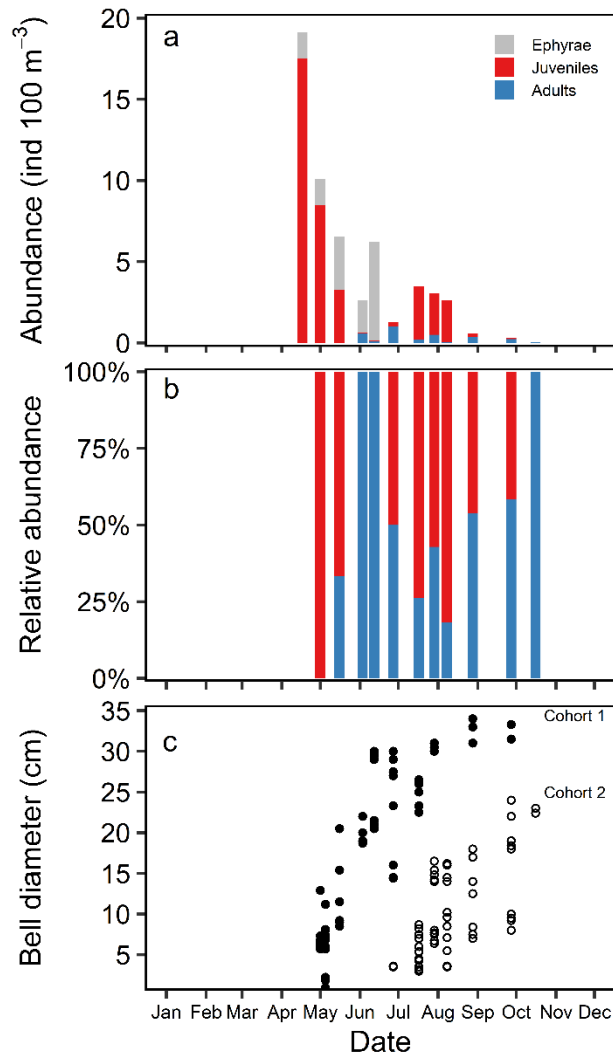
470 Previous studies have analyzed a limited medusae size range or have only focused on one  
471 developmental stage (Costello & Colin, 1994; Álvarez-Tello et al., 2016; Milisenda et al., 2018). Because  
472 of this, interspecific comparisons on trophic changes, diet compositions, and selectivity patterns should  
473 be made with caution, as a wide variety of methodologies and medusae sizes have been used. We stress  
474 the need for a standardization of methods (e.g., Nagata & Morandini, 2018) to assess trophic dietary  
475 niches of jellyfish that will allow to identify feeding patterns or latitudinal changes, which are not  
476 achievable with current knowledge.



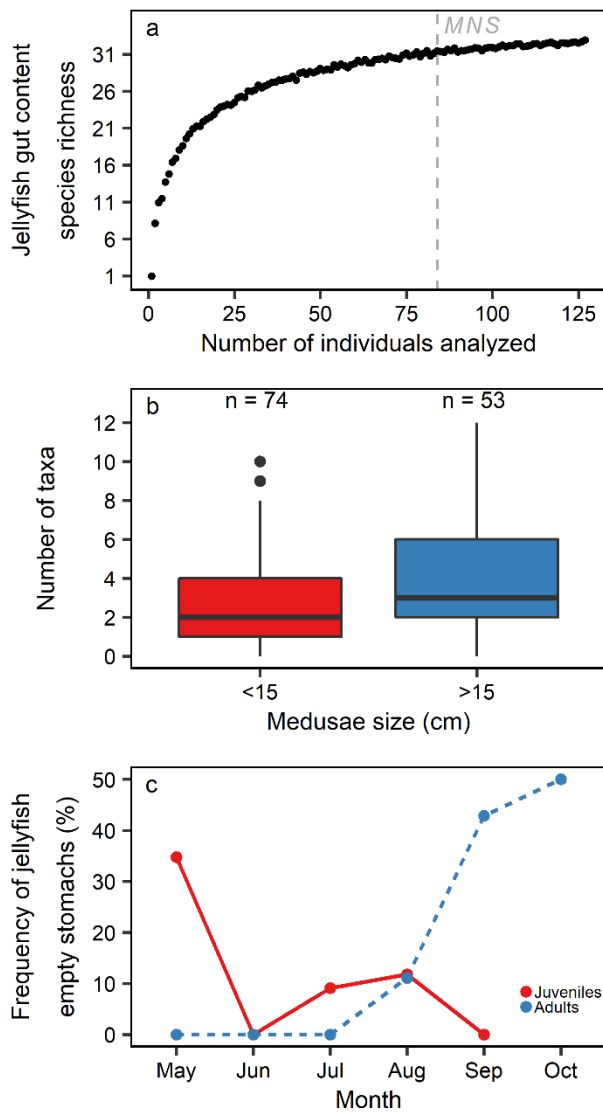
477 **Conclusions**

478 Rhizostomeae jellyfish are an important component of the coastal ecosystems, but the dietary niche of  
479 most of the species (ca. 85%) remains unknown and therefore their trophic role in food webs. Here, we  
480 identified that medusae of *R. pulmo* do not feed on the same prey during ontogeny, providing evidence  
481 that this jellyfish modifies its trophodynamics, as other marine animals such as bony fish (Olson, 1996;  
482 Costalago et al., 2012), sharks (Bethea et al., 2007), sea turtles (Vélez-Rubio et al., 2016) and marine  
483 mammals (Vales et al., 2014). Since *R. pulmo* appear seasonally on most Mediterranean coasts for  
484 approximately 7 months (Leoni et al., 2021a), its predatory impact on the planktonic community should  
485 be temporally restricted and variable depending on the stage of development, abundances, and prey  
486 densities. Here, we provide the first *in situ* estimations of their predatory impact in natural ecosystems.  
487 The inclusion of indirect techniques as SI and FA analyses will help to elucidate if some other prey items  
488 are neglected by the visual analysis method. Metabarcoding techniques have also proved to be useful in  
489 diet composition identification for marine animals (Berry et al., 2015; Bergmann et al., 2021), and should  
490 be considered in future analyses of the diet of Rhizostomeae. Our study provides a baseline for  
491 understanding the trophic role of this species, and therefore for its better representation in food web  
492 models.

493

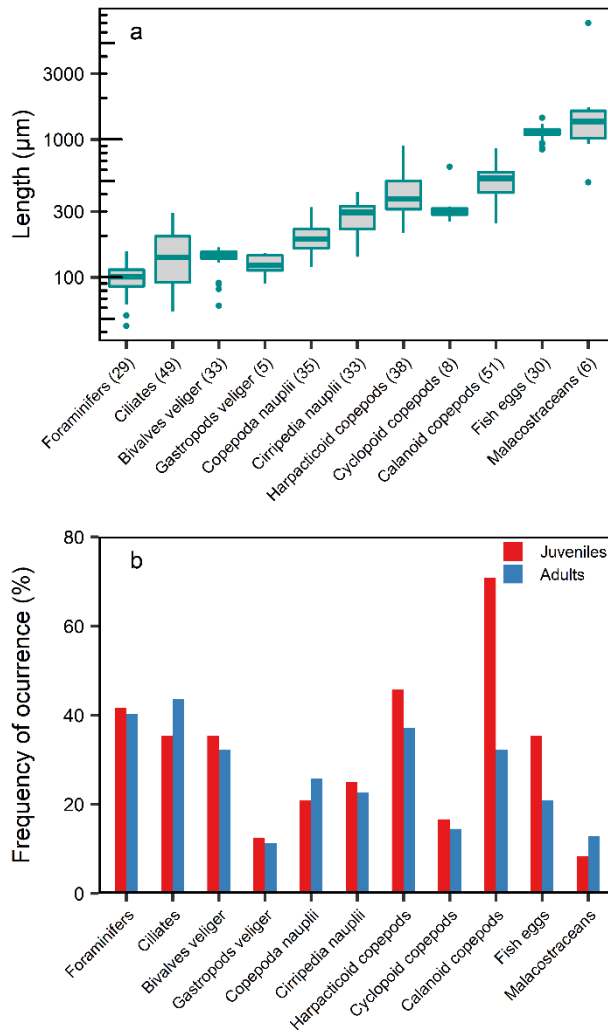


497 **Figure 1. a.** Total abundance (ind 100 m<sup>-3</sup>) of the pelagic stage of *Rhizostoma pulmo* estimated during 2019 in  
 498 Bages Sigean lagoon (France). Abundance for each developmental stage is indicated in colors: ephyrae in grey,  
 499 juveniles (bell diameter <15 cm) in red and adults (bell diameter >15 cm) in blue. **b.** Relative abundance (%) of  
 500 juveniles (red) and adults (blue) stages of *R. pulmo* collected for gut content analysis, and **c.** bell diameter (cm) of  
 501 medusae collected for gut content analysis by sampling date. Full dots are the individuals from the first cohort and  
 502 empty dots are the individuals from the second cohort.



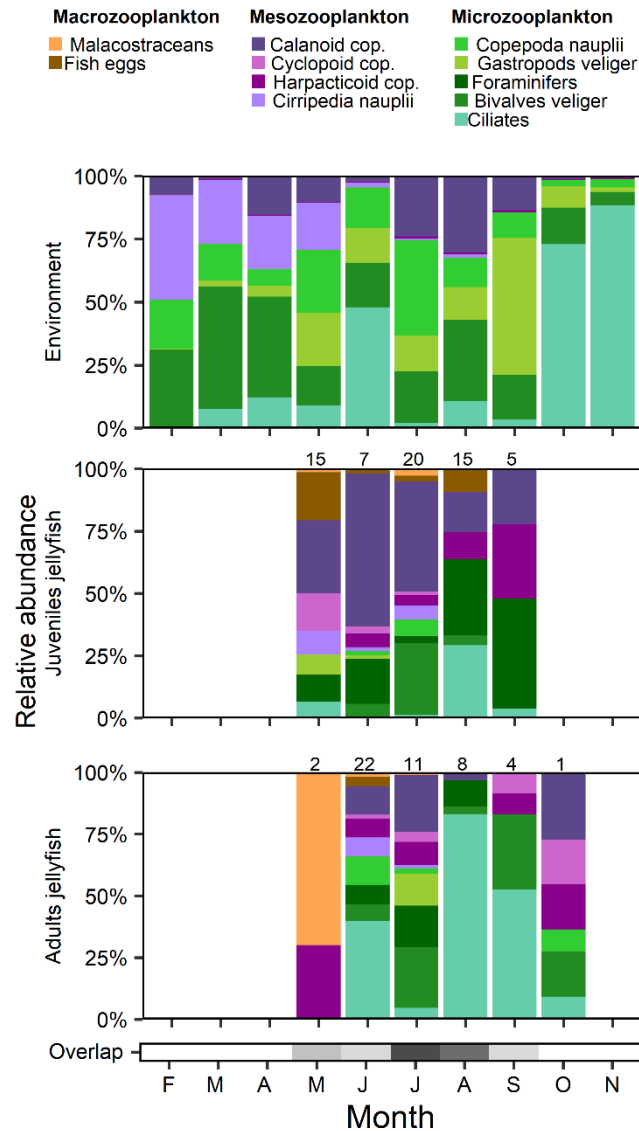
503

504 **Figure 2. a.** Rarefaction curve for prey species richness indicating the required sampling effort to avoid unbiased  
 505 *Rhizostoma pulmo* medusa diet determination. In the present study, the minimum number of guts (*MNS*) to  
 506 represent prey richness was 84 (grey dashed line). The cumulative curve was calculated using the content of each  
 507 medusa gut as a sampling unit (n=127). **b.** Number of taxa observed in the gut content of juveniles (bell diameter  
 508 <15 cm) and adults (bell diameter >15 cm) specimens of *R. pulmo* (Kruskal-Wallis  $\chi^2=7.38$ ,  $df=1$ ,  $p=0.007$ ). **c.**  
 509 Frequency of medusae empty guts (%) by stage of development (juveniles, represented by a red continuous line,  
 510 and adults represented by a blue dotted line).  
 511



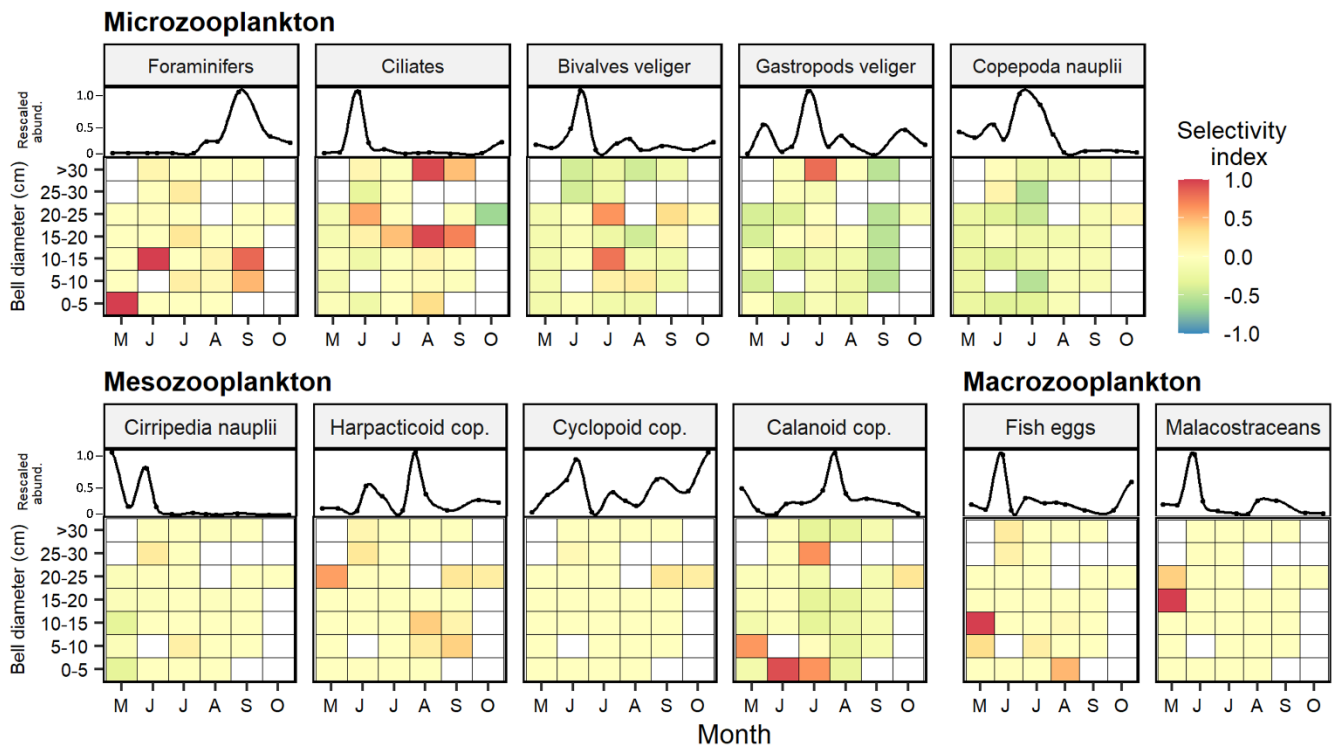
512

513 **Figure 3. a.** Size (µm) of the different zooplankton prey items in the gut content of *Rhizostoma pulmo* (n=110)  
 514 during 2019 in Bages Sigean lagoon (France). Numbers in parenthesis indicate the prey specimens measured. Note  
 515 that the ‘Y’ axis is represented in a logarithmic scale. **b.** Frequency of occurrence of the different prey items in the  
 516 gut content of juvenile (bell diameter <15 cm, in red) and adult (bell diameter >15 cm, in blue) medusae of *R.*  
 517 *pulmo*.  
 518



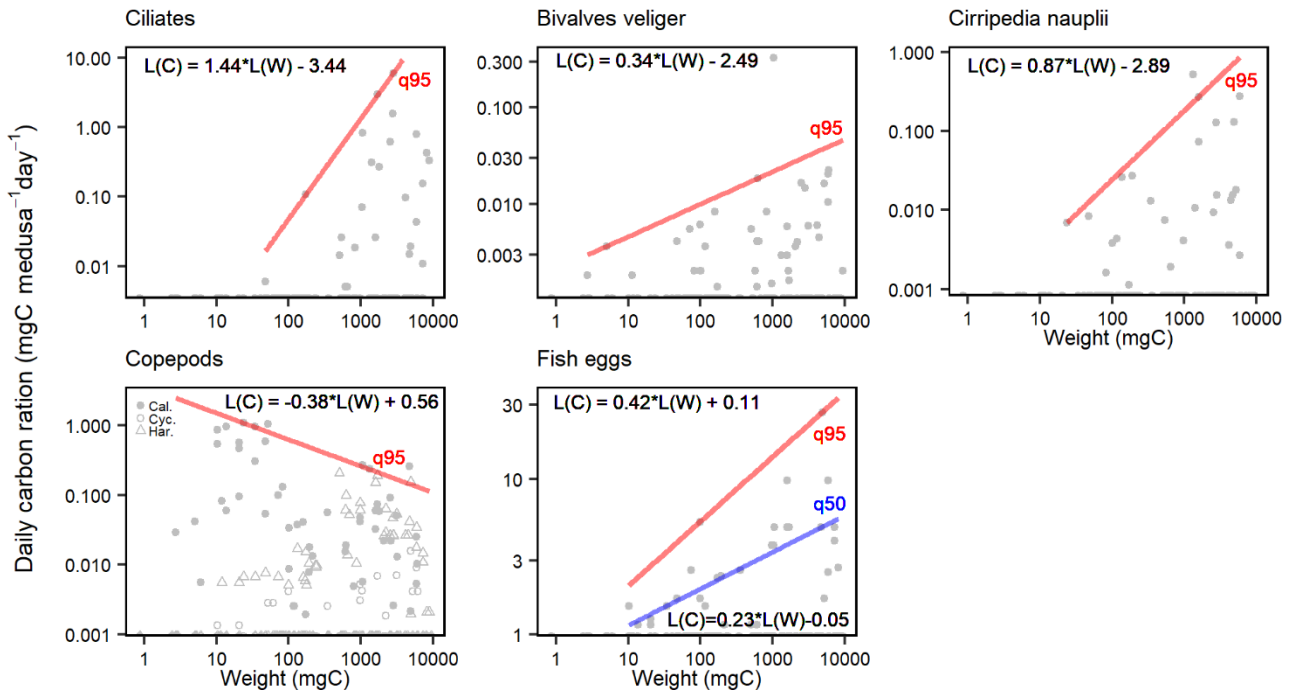
519

520 **Figure 4.** Monthly relative abundance (%) of each taxon observed in Bages Sigean lagoon (France) (top) from  
 521 February to November 2019, and in the gut content of *Rhizostoma pulmo* medusae juveniles (center) and adults  
 522 (bottom) from May to October 2019 for the three size categories: Macrozooplankton (>700  $\mu\text{m}$ , in orange scale:  
 523 malacostraceans and fish eggs), mesozooplankton (200-700  $\mu\text{m}$ , in purple scale: Calanoid, cyclopoid and  
 524 harpacticoid copepods, and Cirripedia nauplii) and microzooplankton (63-200  $\mu\text{m}$ , in green scale: Copepoda  
 525 nauplii, gastropods and bivalves veliger, foraminifers and ciliates). Note the temporal variability in the number of  
 526 medusae analyzed by month (numbers on top). Niche overlap between juveniles and adults is represented at the  
 527 bottom, only for months with juveniles and adults coexisting (from May to September). Scale from 0 to 100%,  
 528 with 0% (white) representing no diet overlap, and 100% (black) identical diets.  
 529



530  
531  
532  
533  
534  
535  
536  
537

**Figure 5.** Selectivity index (*LFSI*) for zooplankton prey per month according to *Rhizostoma pulmo* medusa size. Prey taxa are grouped by size on microzooplankton (63-200  $\mu\text{m}$ ), mesozooplankton (200-700  $\mu\text{m}$ ) and macrozooplankton ( $>700 \mu\text{m}$ ). Positive (orange-red) or negative (green-blue) index values indicate selectivity at a rate above or below environmental concentration, respectively. Yellow indicates that dietary composition was similar to the proportional abundances in the surrounding zooplankton. White areas denote no data. Prey abundance seasonal patterns during 2019 in Bages Sigean lagoon (France), rescaled to 0-1, are shown in the top panel of each plot.



538

539 **Figure 6.** Daily Carbon Ration (mgC consumed medusa<sup>-1</sup> day<sup>-1</sup>) from *Rhizostoma pulmo* gut content in relation  
 540 with the medusae weight (in mgC). Each point represents one medusa and regression lines the quantile 50% (blue)  
 541 and 95% (red). Only the statistical significant regressions (p<0.05) are represented. Equations correspond to the  
 542 quantile regressions between log<sub>10</sub> Daily Carbon Ration (L(C) in mgC medusa<sup>-1</sup> day<sup>-1</sup>) and the log<sub>10</sub> medusae  
 543 weight (L(W) in mgC). ‘X’ and ‘Y’ axis are represented in logarithmic scale. Note that the ‘Y’ axis scale differs  
 544 among taxa. Cal.=Calanoid, Cyc=Cyclopoid, Har=Harpacticoid.

545 **Acknowledgements**

546 This study was conducted as part of the Ph.D. dissertation of V.L. and was supported by the National  
547 Agency for Research and Innovation, ANII, Uruguay (code POS\_CFRA\_2017\_1\_147109). Part of the  
548 analyses were financed by EMBRC-France, a program managed by the ANR within the “Investing for  
549 the future program” under the reference ANR-10-INBS-02. The authors acknowledge the funding  
550 support of the French ANR project CIGOEF (grant ANR-17-CE32-0008-01), and the support of LabEx  
551 CeMEB, an ANR "Investissements d'avenir" program (ANR - 10 - LABX - 04 - 01). We acknowledge  
552 Sun Hee Lee, Ruben Tournier and Raquel Marques for their assistance during fieldwork. We greatly  
553 appreciated the advice from Renato M. Nagata for laboratory manipulations and the advice from  
554 Alejandro Ariza for graphic designs. We are grateful to the kitesurf center ‘Narbonne Kite Passion’ and  
555 local fishermen for the logistic support, in particular to the skipper Stéphane Marin, for his support on  
556 board and for sharing his expertise on the lagoon. We would like to thank the reviewers and the associated  
557 editor of the previous version of this manuscript, whose comments greatly improved the quality of the  
558 present manuscript.



559 **References**

- 560 Álvarez-Tello, F. J., J. López-Martínez, & D. B. Lluch-Cota, 2016. Trophic spectrum and feeding  
561 pattern of cannonball jellyfish *Stomolophus meleagris* (Agassiz, 1862) from central Gulf of California.  
562 *Journal of the Marine Biological Association of the United Kingdom* 96: 1217–1227.
- 563 Ballesteros, A., C. Östman, A. Santín, M. Marambio, M. Narda, & J.-M. Gili, 2021. Cnidome and  
564 morphological features of *Pelagia noctiluca* (Cnidaria: Scyphozoa) throughout the different life cycle  
565 stages. *Frontiers in Marine Science* 8: 714503.
- 566 Båmstedt, U., & M. B. Martinussen, 2000. Estimating digestion rate and the problem of individual  
567 variability, exemplified by a scyphozoan jellyfish. *Journal of Experimental Marine Biology and*  
568 *Ecology* 251: 1–15.
- 569 Basso, L., L. Rizzo, M. Marzano, M. Intranuovo, B. Fosso, G. Pesole, S. Piraino, & L. Stabili, 2019.  
570 Jellyfish summer outbreaks as bacterial vectors and potential hazards for marine animals and humans  
571 health? The case of *Rhizostoma pulmo* (Scyphozoa, Cnidaria). *Science of The Total Environment* 692:  
572 305–318.
- 573 Bergmann, M. P. M. van Z., B. D. Postaire, K. Gastrich, M. R. Heithaus, L. A. Hoopes, K. Lyons, Y. P.  
574 Papastamatiou, E. V. C. Schneider, B. A. Strickland, B. S. Talwar, D. D. Chapman, & J. Bakker, 2021.  
575 Elucidating shark diets with DNA metabarcoding from cloacal swabs. *Molecular Ecology Resources*  
576 21: 1056–1067.
- 577 Berry, O., C. Bulman, M. Bunce, M. Coghlan, D. C. Murray, & R. D. Ward, 2015. Comparison of  
578 morphological and DNA metabarcoding analyses of diets in exploited marine fishes. *Marine Ecology*  
579 *Progress Series* 540: 167–181.
- 580 Bethea, D. M., L. Hale, J. K. Carlson, E. Cortés, C. A. Manire, & J. Gelsleichter, 2007. Geographic and  
581 ontogenetic variation in the diet and daily ration of the bonnethead shark, *Sphyrna tiburo*, from the  
582 eastern Gulf of Mexico. *Marine Biology* 152: 1009–1020.
- 583 Bonnet, D., 2013. Etude du plancton gélatineux sur la façade Méditerranéenne- GELAMED-  
584 Programme Liteau (189)- rapport d'activités. , [http://docplayer.fr/106255915-Gelamed-etude-du-](http://docplayer.fr/106255915-Gelamed-etude-du-plancton-gelatineux-sur-la-facade-mediterraneenne.html)  
585 [plancton-gelatineux-sur-la-facade-mediterraneenne.html](http://docplayer.fr/106255915-Gelamed-etude-du-plancton-gelatineux-sur-la-facade-mediterraneenne.html).
- 586 Bosch-Belmar, M., G. Milisenda, L. Basso, T. K. Doyle, A. Leone, & S. Piraino, 2021. Jellyfish  
587 impacts on marine aquaculture and fisheries. *Reviews in Fisheries Science & Aquaculture* 29: 242–259.
- 588 Brodeur, R., H. Sugisaki, & G. Hunt, 2002. Increases in jellyfish biomass in the Bering Sea:  
589 implications for the ecosystem. *Marine Ecology Progress Series* 233: 89–103.
- 590 Cade, B. S., & B. R. Noon, 2003. A gentle introduction to quantile regression for ecologists. *Frontiers*  
591 *in Ecology and the Environment* 1: 412–420.
- 592 Calder, D. R., 1983. Nematocysts of stages in the life cycle of *Stomolophus meleagris*, with keys to  
593 scyphistomae and ephyrae of some western Atlantic Scyphozoa. *Canadian Journal of Zoology* 61:  
594 1185–1192.

- 595 Carr, E. F., & K. A. Pitt, 2008. Behavioural responses of zooplankton to the presence of predatory  
596 jellyfish. *Journal of Experimental Marine Biology and Ecology* 354: 101–110.
- 597 Carrette, T., P. Alderslade, & J. Seymour, 2002. Nematocyst ratio and prey in two Australian  
598 cubomedusans, *Chironex fleckeri* and *Chiropsalmus* sp. *Toxicon* 40: 1547–1551.
- 599 Cesmat, L., K. Dusserre, A. Fiandrino, & L. Benau, 2012. Etude hydrologique de l'étang de Bages-  
600 Sigean. Impact de différents scénarii d'aménagement et de gestion sur les variations de salinité. Agence  
601 de l'eau, Conservatoire des Espaces Naturels du Languedoc-Roussillon, Parc Naturel Régional de la  
602 Narbonnaise en Méditerranée, Ifremer, France: 84.
- 603 Chao, A., R. K. Colwell, C.-W. Lin, & N. J. Gotelli, 2009. Sufficient sampling for asymptotic minimum  
604 species richness estimators. *Ecology* 90: 1125–1133.
- 605 Costalago, D., J. Navarro, I. Álvarez-Calleja, & I. Palomera, 2012. Ontogenetic and seasonal changes  
606 in the feeding habits and trophic levels of two small pelagic fish species. *Marine Ecology Progress  
607 Series* 460: 169–181.
- 608 Costello, J. H., & S. P. Colin, 1994. Morphology, fluid motion and predation by the scyphomedusa  
609 *Aurelia aurita*. *Marine Biology* 121: 327–334.
- 610 Costello, J. H., & S. P. Colin, 1995. Flow and feeding by swimming scyphomedusae. *Marine Biology*  
611 124: 399–406.
- 612 Cury, P., Y. Shin, B. Planque, J. Durant, J. Fromentin, S. Kramerschadt, N. Stenseth, M. Travers, & V.  
613 Grimm, 2008. Ecosystem oceanography for global change in fisheries. *Trends in Ecology & Evolution*  
614 23: 338–346.
- 615 da Silveira, E. L., N. Semmar, J. E. Cartes, V. M. Tuset, A. Lombarte, E. L. C. Ballester, & A. M. Vaz-  
616 dos-Santos, 2020. Methods for trophic ecology assessment in fishes: A critical review of stomach  
617 analyses. *Reviews in Fisheries Science & Aquaculture* 28: 71–106.
- 618 Damian-Serrano, A., S. H. D. Haddock, & C. W. Dunn, 2021. The evolution of siphonophore tentilla  
619 for specialized prey capture in the open ocean. *Proceedings of the National Academy of Sciences*  
620 *National Academy of Sciences* 118: 1–9.
- 621 Dawson, M. N., & W. M. Hamner, 2009. A character-based analysis of the evolution of jellyfish  
622 blooms: adaptation and exaptation. *Hydrobiologia* 616: 193–215.
- 623 Dönmez, M. A., & L. Bat, 2019. Detection of feeding dietary *Rhizostoma pulmo* (Macri, 1778) in  
624 Samsun coasts of the Black Sea, Turkey. *Ege Journal of Fisheries and Aquatic Sciences* 36: 135–144.
- 625 Fleming, N. E. C., C. Harrod, J. Newton, & J. D. R. Houghton, 2015. Not all jellyfish are equal:  
626 isotopic evidence for inter- and intraspecific variation in jellyfish trophic ecology. *PeerJ* 3: 1–21.
- 627 Fuentes, V., I. Straehler-Pohl, D. Atienza, I. Franco, U. Tilves, M. Gentile, M. Acevedo, A. Olariaga, &  
628 J. M. Gili, 2011. Life cycle of the jellyfish *Rhizostoma pulmo* (Scyphozoa: Rhizostomeae) and its  
629 distribution, seasonality and inter-annual variability along the Catalan coast and the Mar Menor (Spain,  
630 NW Mediterranean). *Marine Biology* 158: 2247–2266.

- 631 Graham, W. M., & R. M. Kroutil, 2001. Size-based prey selectivity and dietary shifts in the jellyfish,  
632 *Aurelia aurita*. *Journal of Plankton Research* 23: 67–74.
- 633 Graham, W. M., D. L. Martin, D. L. Felder, V. L. Asper, & H. M. Perry, 2003. Ecological and economic  
634 implications of a tropical jellyfish invader in the Gulf of Mexico. *Marine Bioinvasions: Patterns,*  
635 *Processes and Perspectives* 53–69.
- 636 Granéli, E., & J. Turner, 2002. Top-down regulation in ctenophore-copepod-ciliate-diatom-  
637 phytoflagellate communities in coastal waters: a mesocosm study. *Marine Ecology Progress Series* 239:  
638 57–68.
- 639 Gueroun, S. K. M., J. C. Molinero, S. Piraino, & M. N. D. Yahia, 2020. Population dynamics and  
640 predatory impact of the alien jellyfish *Aurelia solida* (Cnidaria, Scyphozoa) in the Bizerte Lagoon  
641 (southwestern Mediterranean Sea). *Mediterranean Marine Science* 21: 22–35.
- 642 Hays, G. C., T. Bastian, T. K. Doyle, S. Fossette, A. C. Gleiss, M. B. Gravenor, V. J. Hobson, N. E.  
643 Humphries, M. K. S. Lilley, N. G. Pade, & D. W. Sims, 2012. High activity and Levy searches:  
644 jellyfish can search the water column like fish. *Proceedings of the Royal Society B: Biological*  
645 *Sciences* 279: 465–473.
- 646 Hays, G. C., T. K. Doyle, & J. D. R. Houghton, 2018. A paradigm shift in the trophic importance of  
647 jellyfish?. *Trends in Ecology & Evolution* 33: 874–884.
- 648 Hecq, J. H., A. Collignon, & A. Goffart, 2014. Atlas du zooplancton des eaux côtières corses. Travail  
649 de synthèse réalisé à la demande de l'Agence de l'Eau RMC, France,  
650 <http://orbi.ulg.ac.be/handle/2268/168>.
- 651 Hyslop, J. F., 1980. Stomach content analysis-a review on methods and their application. *Journal of*  
652 *Fish Biology* 17: 411–429.
- 653 Jiménez-Valverde, A., & J. Hortal, 2003. Las curvas de acumulación de especies y la necesidad de  
654 evaluar la calidad de los inventarios biológicos. *Revista Ibérica de Aracnología* 8: 151–161.
- 655 Kikinger, R., 1992. *Cotylorhiza tuberculata* (Cnidaria: Scyphozoa) - Life history of a stationary  
656 population. *Marine Ecology* 13: 333–362.
- 657 Krebs, C. J., 1999. *Ecological methodology*. Benjamin Cummings, New York.
- 658 Kuplik, Z., & D. L. Angel, 2020. Diet composition and some observations on the feeding ecology of  
659 the rhizostome *Rhopilema nomadica* in Israeli coastal waters. *Journal of the Marine Biological*  
660 *Association of the United Kingdom* 100: 681–689.
- 661 Langton, R. W., 1982. Diet overlap between Atlantic cod, *Gadus morhua*, silver hake, *Merluccius*  
662 *bilinearis*, and fifteen other northwest Atlantic finfish. *Fishery Bulletin* 80: 16.
- 663 Larson, R. J., 1991. Diet, prey selection and daily ration of *Stomolophus meleagris*, a filter-feeding  
664 scyphomedusa from the NE Gulf of Mexico. *Estuarine, Coastal and Shelf Science* 32: 511–525.

- 665 Lebrato, M., M. Pahlow, J. R. Frost, M. Küter, P. Jesus Mendes, J. Molinero, & A. Oschlies, 2019.  
666 Sinking of gelatinous zooplankton biomass increases deep carbon transfer efficiency globally. *Global*  
667 *Biogeochemical Cycles* 33: 1764–1783.
- 668 Leoni, V., D. Bonnet, E. Ramírez - Romero, & J. C. Molinero, 2021a. Biogeography and phenology of  
669 the jellyfish *Rhizostoma pulmo* (Cnidaria: Scyphozoa) in southern European seas. *Global Ecology and*  
670 *Biogeography* 30: 622–639.
- 671 Leoni, V., J. C. Molinero, M. Meffre, & D. Bonnet, 2021b. Variability of growth rates and thermohaline  
672 niches of *Rhizostoma pulmo*'s pelagic stages (Cnidaria: Scyphozoa). *Marine Biology* 168: 107.
- 673 Lilley, M. K. S., J. D. R. Houghton, & G. C. Hays, 2009. Distribution, extent of inter-annual variability  
674 and diet of the bloom-forming jellyfish *Rhizostoma* in European waters. *Journal of the Marine*  
675 *Biological Association of the United Kingdom* 89: 39.
- 676 Lucas, C. H., D. O. B. Jones, C. J. Hollyhead, R. H. Condon, C. M. Duarte, W. M. Graham, K. L.  
677 Robinson, K. A. Pitt, M. Schildhauer, & J. Regetz, 2014. Gelatinous zooplankton biomass in the global  
678 oceans: geographic variation and environmental drivers. *Global Ecology and Biogeography* 23: 701–  
679 714.
- 680 Marques, R., D. Bonnet, C. Carré, C. Roques, & A. M. Darnaude, 2021. Trophic ecology of a blooming  
681 jellyfish (*Aurelia coerulea*) in a Mediterranean coastal lagoon. *Limnology and Oceanography* 66: 141–  
682 157.
- 683 Milisenda, G., S. Rossi, S. Vizzini, V. L. Fuentes, J. E. Purcell, U. Tilves, & S. Piraino, 2018. Seasonal  
684 variability of diet and trophic level of the gelatinous predator *Pelagia noctiluca* (Scyphozoa). *Scientific*  
685 *Reports* 8: 12140.
- 686 Moore, M. V., B. T. De Stasio, K. N. Huizenga, & E. A. Silow, 2019. Trophic coupling of the microbial  
687 and the classical food web in Lake Baikal, Siberia. *Freshwater Biology* 64: 138–151.
- 688 Nagata, R. M., & A. C. Morandini, 2018. Diet, prey selection, and individual feeding rates of the  
689 jellyfish *Lychnorhiza lucerna* (Scyphozoa, Rhizostomeae). *Marine Biology* 165: 187.
- 690 Nagata, R., A. Morandini, S. Colin, A. Migotto, & J. Costello, 2016. Transitions in morphologies, fluid  
691 regimes, and feeding mechanisms during development of the medusa *Lychnorhiza lucerna*. *Marine*  
692 *Ecology Progress Series* 557: 145–159.
- 693 Nagata, R., M. Moreira, C. Pimentel, & A. Morandini, 2015. Food web characterization based on  $\delta^{15}\text{N}$   
694 and  $\delta^{13}\text{C}$  reveals isotopic niche partitioning between fish and jellyfish in a relatively pristine ecosystem.  
695 *Marine Ecology Progress Series* 519: 13–27.
- 696 Nastav, B., M. Malej, A. Malej Jr., & A. Malej, 2013. Is it possible to determine the economic impact of  
697 jellyfish outbreaks on fisheries? A case study – Slovenia. *Mediterranean Marine Science* 14: 214.
- 698 Oba, A., M. Hidaka, & S. Iwanaga, 2004. Nematocyst composition of the cubomedusan *Chiropsalmus*  
699 *quadrigatus* changes with growth. *Hydrobiologia* 530/531: 173–177.
- 700 Olson, M. H., 1996. Ontogenetic niche shifts in Largemouth Bass: Variability and consequences for  
701 first-year growth. *Ecology* 77: 179–190.

- 702 Padilla-Serrato, J. G., J. López-Martínez, A. Acevedo-Cervantes, E. Alcántara-Razo, & C. H. Rábago-  
703 Quiroz, 2013. Feeding of the scyphomedusa *Stomolophus meleagris* in the coastal lagoon Las  
704 Guásimas, northwest Mexico. 23: 9.
- 705 Pauly, D., W. M. Graham, S. Libralato, L. Morissette, & M. L. D. Palomares (eds), 2009. Jellyfish in  
706 ecosystems, online databases, and ecosystem models. *Hydrobiologia* 616: 67–85.
- 707 Pérez-Ruzafa, A., J. Gilabert, J. M. Gutiérrez, A. I. Fernández, C. Marcos, & S. Sabah, 2002. Evidence  
708 of a planktonic food web response to changes in nutrient input dynamics in the Mar Menor coastal  
709 lagoon, Spain. *Hydrobiologia* 359–369.
- 710 Pitt, K. A., R. M. Connolly, & J. E. Purcell, 2009. Stable isotope and fatty acid tracers in energy and  
711 nutrient studies of jellyfish: a review. 616: 119–132.
- 712 Pitt, K. A., & C. H. Lucas (eds), 2013. Jellyfish blooms. Springer, Dordrecht.
- 713 PNRNM, 2018. Réhabilitation et valorisation de l'étang de Bages-Sigean. Les Zones Humides. ,  
714 [http://www.zones-humides.org/agir/retours-experiences/rehabilitation-et-valorisation-de-l039etang-de-](http://www.zones-humides.org/agir/retours-experiences/rehabilitation-et-valorisation-de-l039etang-de-bages-sigean)  
715 [bages-sigean](http://www.zones-humides.org/agir/retours-experiences/rehabilitation-et-valorisation-de-l039etang-de-bages-sigean).
- 716 Purcell, J., 1992. Effects of predation by the scyphomedusan *Chrysaora quinquecirrha* on zooplankton  
717 populations in Chesapeake Bay, USA. *Marine Ecology Progress Series* 87: 65–76.
- 718 Purcell, J. E., 1984. The functions of nematocysts in prey capture by epipelagic siphonophores  
719 (Coelenterata, Hydrozoa). *The Biological Bulletin* 166: 310–327.
- 720 Purcell, J. E., 1997. Pelagic cnidarians and ctenophores as predators: Selective predation, feeding rates,  
721 and effects on prey populations. *Annales de l'Institut océanographique* 73: 125–137.
- 722 Purcell, J. E., 2003. Predation on zooplankton by large jellyfish, *Aurelia labiata*, *Cyanea capillata* and  
723 *Aequorea aequorea*, in Prince William Sound, Alaska. *Marine Ecological Progress Series* 16.
- 724 Purcell, J. E., 2009. Extension of methods for jellyfish and ctenophore trophic ecology to large-scale  
725 research. *Hydrobiologia* 616: 23–50.
- 726 Purcell, J. E., 2018. Of jellyfish, fish, and humans. *ICES Journal of Marine Science* 75: 1235–1244.
- 727 Purcell, J. E., V. Fuentes, D. Atienza, U. Tilves, D. Astorga, M. Kawahara, & G. C. Hays, 2010. Use of  
728 respiration rates of scyphozoan jellyfish to estimate their effects on the food web. *Hydrobiologia* 645:  
729 135–152.
- 730 Purcell, J. E., & C. E. Mills, 1988. The correlation between nematocyst types and diets in pelagic  
731 Hydrozoa In Hessinger, D. A., & H. M. Lenhoff (eds), *The Biology of Nematocysts*. Academic Press:  
732 464–483.
- 733 R Core Team, 2020. R: A language and environment for statistical computing. R Foundation for  
734 Statistical Computing, Vienna, Austria, <https://www.R-project.org/>.
- 735 Regula, C., S. Colin, J. Costello, & H. Kordula, 2009. Prey selection mechanism of ambush-foraging  
736 hydromedusae. *Marine Ecology Progress Series* 374: 135–144.

- 737 Robinson, K., & W. Graham, 2014. Warming of subtropical coastal waters accelerates *Mnemiopsis*  
738 *leidyi* growth and alters timing of spring ctenophore blooms. Marine Ecology Progress Series 502:  
739 105–115.
- 740 Rosa, S., M. Pansera, A. Granata, & L. Guglielmo, 2013. Interannual variability, growth, reproduction  
741 and feeding of *Pelagia noctiluca* (Cnidaria: Scyphozoa) in the Straits of Messina (Central  
742 Mediterranean Sea): Linkages with temperature and diet. Journal of Marine Systems 111–112: 97–107.
- 743 Rossi, J. P., 2011. rich: an R package to analyse species richness. Diversity 3: 112–120.
- 744 Sánchez-Hernández, J., A. D. Nunn, C. E. Adams, & P.-A. Amundsen, 2019. Causes and consequences  
745 of ontogenetic dietary shifts: a global synthesis using fish models: Ontogenetic dietary shifts.  
746 Biological Reviews 94: 539–554.
- 747 Sieracki, C., M. Sieracki, & C. Yentsch, 1998. An imaging-in-flow system for automated analysis of  
748 marine microplankton. Marine Ecology Progress Series 168: 285–296.
- 749 Strauss, R. E., 1979. Reliability estimates for Ivlev's electivity index, the forage ratio, and a proposed  
750 linear index of food selection. Transactions of the American Fisheries Society 108: 344–352.
- 751 Syazwan, W. M., A. Y.-H. Then, V. C. Chong, & M. Rizman-Idid, 2021. Trophic ecology of a tropical  
752 scyphozoan community in coastal waters: Insights from stomach content and stable isotope analyses.  
753 Continental Shelf Research 225: 104481.
- 754 Trégouboff, G., & M. Rose, 1978. Manuel de planctonologie méditerranéenne. France.
- 755 Turk, V., D. Lučić, V. Flander-Putrlje, & A. Malej, 2008. Feeding of *Aurelia* sp. (Scyphozoa) and links  
756 to the microbial food web. Marine Ecology 29: 495–505.
- 757 Uye, S., 1982. Length-weight relationships of important zooplankton from the Inland Sea of Japan.  
758 Journal of the Oceanographical Society of Japan 38: 149–158.
- 759 Uye, S., 2008. Blooms of the giant jellyfish *Nemopilema nomurai*: a threat to the fisheries  
760 sustainability of the East Asian Marginal Seas. Plankton and Benthos Research 3: 125–131.
- 761 Vales, D. G., F. Saporiti, L. Cardona, L. R. De Oliveira, R. A. Dos Santos, E. R. Secchi, A. Aguilar, &  
762 E. A. Crespo, 2014. Intensive fishing has not forced dietary change in the South American fur seal  
763 *Arctophoca* (= *Arctocephalus*) *australis* off Río de la Plata and adjoining areas. Aquatic Conservation:  
764 Marine and Freshwater Ecosystems 24: 745–759.
- 765 Vélez-Rubio, G. M., L. Cardona, M. López-Mendilaharsu, G. Martínez Souza, A. Carranza, D.  
766 González-Paredes, & J. Tomás, 2016. Ontogenetic dietary changes of green turtles (*Chelonia mydas*) in  
767 the temperate southwestern Atlantic. Marine Biology 163: 57.
- 768 Wagner, Z., J. H. Costello, & S. P. Colin, 2020. Fluid and Predator-Prey Interactions of Scyphomedusae  
769 Fed Calanoid Copepods. Fluids 5: 60.
- 770 Wang, P., F. Zhang, M. Liu, S. Sun, & H. Xian, 2020. Isotopic evidence for size-based dietary shifts in  
771 the jellyfish *Cyanea nozakii* in the northern East China Sea. Journal of Plankton Research 1–13.

772 West, E. J., K. A. Pitt, D. T. Welsh, K. Koop, & D. Rissik, 2009. Top-down and bottom-up influences of  
773 jellyfish on primary productivity and planktonic assemblages. *Limnology and Oceanography* 54: 2058–  
774 2071.

775 Wickham, H., 2016. *ggplot2: Elegant Graphics for Data Analysis*. Springer International Publishing,  
776 <https://www.springer.com/gp/book/9783319242750>.

777